WEP Warwick Evans Publishing

International Journal of Natural Resources and Environmental Studies

ISSN: 3006-2012 (Print), ISSN: 3006-0834 (Online) | Volume 5, Number 3, Year 2025
DOI: https://doi.org/10.62051/ijnres.v5n3.09
Journal homepage: https://wepub.org/index.php/IJNRES/index

Mechanisms of Elevated Sulfate Concentrations in High Geotemperature Coal Mining Areas

Yuanmeng Li*

School of Resources and Environment Engineering, Henan Polytechnic University, 454000 Jiaozuo, China

*Corresponding Author: Yuanmeng Li

ABSTRACT

Sulfate (SO_4^{2-}) contamination in groundwater within mining areas has garnered widespread global attention, while prolonged coal mining activities have further complicated geological conditions and hydrogeochemical environments. This study investigates the sources and evolution of SO_4^{2-} in the Pingdingshan coal mining area based on multi-year hydrochemical data. Key findings are as follows:Ion correlation analysis demonstrates that cation exchange between Na^+ and Ca^{2+}/Mg^{2+} dominates hydrogeochemical processes in the groundwater; Spatiotemporal sulfate variations, analyzed through hydrochemical data and statistical methods, reveal that sulfate concentrations in the sandstone aquifer exhibit the most significant fluctuations under mining impacts, whereas phreatic and limestone groundwater sulfate concentrations oscillate within a range of 200 mg/L; Comparative analysis between the Pingdingshan (high geotemperature mining area) and Jiaozuo (ambient-temperature mining area) coal regions indicates that elevated geotemperature, water circulation, and water-rock interactions enhance mineral dissolution and sulfide oxidation, leading to anomalously high sulfate concentrations in groundwater; This study elucidates the migration and evolution mechanisms of SO_4^{2-} in the study area, providing critical insights for mitigating sulfate contamination in groundwater systems of high geotemperature coal mining regions in North China.

KEYWORDS

Sulfate; Coal mining groundwater; High geotemperature environment.

1. INTRODUCTION

Groundwater, as a crucial strategic freshwater resource, is characterized by its extensive distribution, abundant reserves (accounting for approximately 99% of global liquid freshwater), high quality, and strong contamination resistance[1]. It plays an irreplaceable role in global drinking water supply and agricultural irrigation[2]. Particularly in the arid and semi-arid regions of northern China, groundwater sustains over 70% of industrial and agricultural water demands[3]. However, with the acceleration of industrialization, this "blue gold" is facing an unprecedented quality crisis. Among these challenges, sulfate pollution, owing to its complex formation mechanisms and significant ecological and health risks, has become a focal research topic in the field of international hydrogeology.

As the world's largest energy consumer, China's unique energy structure has maintained coal's dominant position in the national economy. Data from the National Bureau of Statistics show that in 2020, coal accounted for a proportion of primary energy consumption far exceeding the combined total of petroleum, natural gas, and all renewable energy sources[4]. This energy dependency is particularly pronounced in North China-type coalfields—this region contributes approximately 65% of the nation's coal output, supporting the development of core economic zones such as the Beijing-

Tianjin-Hebei urban agglomeration[5]. With the gradual depletion of shallow resources, coal mining depths are progressively extending to deeper levels[6], and the resulting deep geological environmental effects have become critical bottlenecks constraining sustainable development in mining areas.

Deep mining activities disturb groundwater systems through multiple mechanisms: Coal mining alters aquifer structures, creating hydraulic connectivity between previously isolated aquifers; Mine drainage induces continuous regional groundwater level decline, forming depression cones[7]; Elevated geothermal gradients (averaging 3.5°C/100 m in North China-type coalfields) raise surrounding rock temperatures in mining faces to 45–60°C, significantly modifying water-rock interaction dynamics[8].These perturbations collectively govern sulfate migration and transformation in groundwater: Traditional pathways (e.g., pyrite oxidation and gypsum dissolution) intertwine with deep subsurface processes (e.g., sulfate-reducing bacteria metabolism and hydrothermal alteration), forming a complex sulfur biogeochemical cycling system.

2. STUDY AREA

The surface water bodies in the Pingdingshan coal mining area belong to the tributaries of the Huai River. The Sha River and Ru River flow from west to east along the southwestern and northeastern margins of the mining area, respectively. The Ru River, serving as the primary recharge source for the minefield aquifers, meanders through the mining area and replenishes the overlying gravel-sand aquifer in the upper cover layer via seepage recharge. This is followed by inter-aquifer leakage recharge to the lower gravel-sand aquifer, sandstone fracture-pore water, and carbonate fracture-karst water. In addition to recharge from surface water bodies and atmospheric precipitation infiltration, atmospheric precipitation directly recharges deep groundwater in the western mining area where Cambrian limestone and dolomitic limestone are exposed.

The Pingdingshan coal mining area is bounded by the Xiang-Jia Fault, Jiaxian Fault, Lu-Ye Fault, and Luo-Gang Fault, forming a centrally uplifted fault block. The northeastern boundary of the mining area starts at the Luo-Gang No. 1 Normal Fault and extends northwestward to the Jiaxian Fault. The southern boundary begins at the outcrop belt of the Geng Formation coal seam and extends northeastward to the Xiang-Jia Fault demarcation line. The coal mining area is influenced by the NW-trending Likou Compound Syncline, with secondary folds developed on both limbs. Studies indicate that groundwater circulation in the Pingdingshan coal mining area is controlled by regional faults and folds, forming a closed hydrogeological unit—the Pingdingshan karst water system (Figure 1)[9].

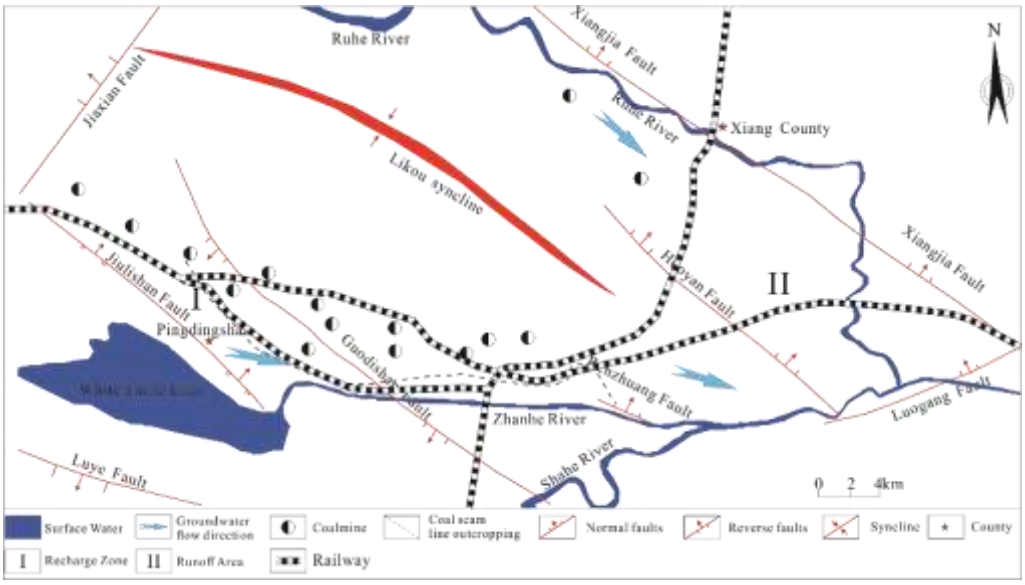

Figure 1. Study Area Overview Map

3. SAMPLE COLLECTION AND ANALYSIS

Portable instruments were employed to measure pH and total dissolved solids (TDS). Prior to sampling, sampling bottles were rinsed 3–4 times with distilled water. Water samples were then filled into the bottles, sealed, and transported to the laboratory. Major hydrochemical ions (Na^+, K^+, Ca^{2+}, etc.) in the water samples were analyzed using an ion chromatograph (SCS-1100), while bicarbonate (HCO_3^-) concentrations were determined via the acid-base titration method[10].

4. RESULTS AND ANALYSIS

4.1. Sources and Influencing Factors of SO_4^{2-}

The cation exchange processes in each aquifer can be observed by analyzing the equivalent ratio of $[Ca^{2+} + Mg^{2+} - SO_4^{2-} - HCO_3^-]/[Na^+ + K^+ - Cl^-]$. A ratio of -1 indicates the occurrence of cation exchange. As shown in Figure 2(a), except for some water samples from the phreatic aquifer, all other samples fall within the fourth quadrant along the line y = -x, demonstrating that cation exchange universally occurs in the mine water of the study area and constitutes the dominant hydrochemical process. Since the mine water in Figure 2(a) lies in the fourth quadrant along y = -x, the original equivalent concentrations of $[Ca^{2+} + Mg^{2+}]$ before cation exchange can be calculated for each aquifer using Equation (4-1). Specifically, the original $[Ca^{2+} + Mg^{2+}]$ equivalents are derived by adding the equivalents of $[Na^+ + K^+ - Cl^-]$ to the measured $[Ca^{2+} + Mg^{2+}]$ equivalents in the solution. Hereafter, the sum $[Ca^{2+} + Mg^{2+} + Na^+ + K^+ - Cl^-]$ is defined as the original equivalent concentration of $[Ca^{2+} + Mg^{2+}]$.

$$Ca2+/Mg2++2（Na/K）X→（Ca/Mg）X2+2Na+/K+ \quad (4\text{-}1)$$

The ratio $[Ca^{2+} + Mg^{2+}]/[SO_4^{2-} + HCO_3^-]$ is commonly used to assess whether hydrogeochemical processes are dominated by the dissolution of carbonate rocks and gypsum. If hydrochemical ions are controlled by carbonate and gypsum dissolution equilibria, data points will align along the dissolution line of carbonate rocks and gypsum (1:1). As shown in Figure 2(b), the original $[Ca^{2+} + Mg^{2+}]/[SO_4^{2-} + HCO_3^-]$ ratios of water samples cluster along the y = x line, indicating that the ions Ca^{2+}, Mg^{2+}, SO_4^{2-}, and HCO_3^- in the mine water of the study area are governed by the dissolution of carbonate rocks and gypsum.

The Ca^{2+} and SO_4^{2-} relationship diagram reflects the gypsum dissolution effect in mine water (Equation 4-2). When the Ca^{2+}/SO_4^{2-} ratio (mmol/L) clusters near the y = x line (1:1), it indicates significant influence from gypsum dissolution. As shown in Figure 2(c), Cambrian limestone groundwater predominantly plots near the gypsum dissolution line, suggesting that sulfate in Cambrian groundwater primarily originates from gypsum dissolution. In contrast, most other mine water samples fall below the gypsum dissolution line, showing negligible gypsum dissolution effects. Jiang et al[11] demonstrated that excess SO_4^{2-} in Pingdingshan mine water is primarily derived from weathering dissolution of sulfate rocks. Therefore, the sources of SO_4^{2-} across aquifers require further investigation.

$$CaSO_4 \cdot 2H2O \rightarrow SO_4^{2-} + Ca^{2+} + H_2O \quad (4\text{-}2)$$

The equivalent ratios $[Ca^{2+} + Mg^{2+}]/HCO_3^-$ and SO_4^{2-}/HCO_3^- can be used to analyze whether H_2SO_4 and H_2CO_3 participate in the dissolution of carbonate rocks in groundwater, as shown in Equations 4-3, 4-4, and 4-5. If the equivalent ratio $[Ca^{2+} + Mg^{2+}]/HCO_3^-$ is 1 and the SO_4^{2-}/HCO_3^- equivalent ratio approaches zero or is very small, it indicates that only H_2CO_3 is involved in the dissolution of carbonate rocks. If the $[Ca^{2+} + Mg^{2+}]/HCO_3^-$ equivalent ratio is 2 and the SO_4^{2-}/HCO_3^- equivalent ratio is 1, it suggests that H_2SO_4 participates in the dissolution of carbonate rocks. If the $[Ca^{2+} + Mg^{2+}]/HCO_3^-$ equivalent ratio is 1.5 and the SO_4^{2-}/HCO_3^- equivalent ratio is 0.5, corresponding to the "+" point in Figure 2(d), it indicates that both H_2SO_4 and H_2CO_3 jointly participate in the dissolution

of carbonate rocks[12]. As shown in Figure 2(d), in the original $[Ca^{2+} + Mg^{2+}]/SO_4^{2-}$ ratios, most mine water samples are distributed near the "+" point, indicating that H_2SO_4 and H_2CO_3 jointly participate in the dissolution of carbonate rocks. Meanwhile, the original $[Ca^{2+} + Mg^{2+}]/HCO_3^-$ ratio continues to increase with the rising SO_4^{2-}/HCO_3^- equivalent ratio, suggesting that sulfuric acid generated from sulfide oxidation under mining disturbances further enhances the dissolution of carbonate rocks. This finding aligns with the analysis by Jiang Xiaofeng et al[13] regarding the sources of sulfate in groundwater from the Pingdingshan mining area.

$$Ca_xMg_{(1-x)}CO_3+H_2CO_3 \rightarrow xCa^{2+}+(1-x)Mg^{2+}+2HCO_3^- \quad (4\text{-}3)$$

$$2Ca_xMg_{(1-x)}CO_3+H_2SO_4 \rightarrow 2xCa^{2+}+2(1-x)Mg^{2+}+SO_4^{2-}+2HCO_3^- \quad (4\text{-}4)$$

$$3Ca_xMg_{(1-x)}CO_3+H_2SO_4+H_2CO_3 \rightarrow 3xCa^{2+}+3(1-x)Mg^{2+}+SO_4^{2-}+4HCO_3^- \quad (4\text{-}5)$$

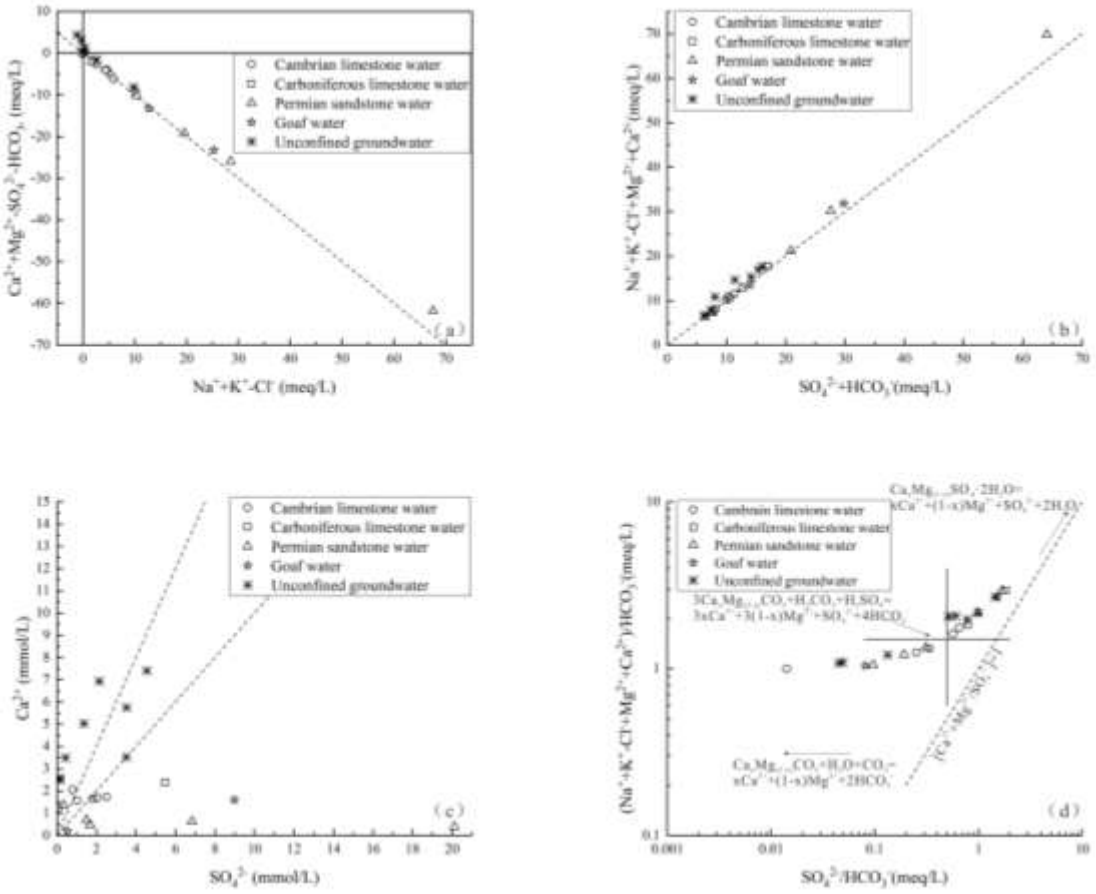

Figure 2. Hydrochemical Ionic Ratios Diagram of the Study Area

Table 1 lists the saturation indices (SI) of gypsum, calcite, and dolomite in mine water (calculated by PHREEQC). Among them, the gypsum saturation indices (SI < -1) indicate high undersaturation, suggesting that gypsum will continue to dissolve in the mine water. Calcite and dolomite in the mine water are in equilibrium and supersaturated states, demonstrating that carbonate mineral dissolution may be a dominant factor influencing the hydrochemical composition of the mine water.

Table 1. Saturation Indices of Gypsum, Dolomite, and Calcite in Mine Groundwater

	SI of Gypsum	SI of Calcite	SI of Dolomite
Cambrain limestone water	-1.72	-0.8	-1.59
	-1.75	-0.18	-0.27
	-1.37	0.03	0.09
	-1.46	-0.19	-0.31
	-1.51	-0.19	-0.37
Carboniferous limestone water	-2.99	0.09	0.21
	-1	0.57	1.02
	-2.25	0.37	0.9
Permian sandstone water	-1.58	0.49	0.59
	-1.6	0.77	1.9
	-2.17	-0.01	0.01
Goaf water	-1.97	0.76	1.54
	-2.91	-0.17	-0.32
	-1.1	0.6	1.33

Figure 3 establishes hydrochemical ionic relationships with saturation indices of gypsum, calcite, and dolomite. In Figure 3(a), the saturation indices of gypsum, calcite, and dolomite increase with rising SO_4^{2-} concentrations, indicating that SO_4^{2-} in mine water is influenced by the dissolution of carbonate rocks and gypsum. In Figure 3(b), as Ca^{2+} concentrations increase, the saturation index of gypsum exhibits an upward trend, while those of dolomite and calcite show a downward trend, suggesting that cation exchange reduces Ca^{2+} in mine water, thereby accelerating gypsum dissolution. Ding et al[14] found that saturation indices of minerals such as gypsum decrease with increasing burial depth in the Pingdingshan mining area. However, as shown in Figure 3(b), the saturation index of gypsum increases with aquifer depth (from the Permian to Cambrian strata). This phenomenon arises because mining activities disrupt the reducing environment, triggering sulfide oxidation in the aquifer and generating H_2SO_4. Simultaneously, intense cation exchange adsorption reduces Ca^{2+} concentrations, further accelerating gypsum dissolution and driving its saturation index toward equilibrium.

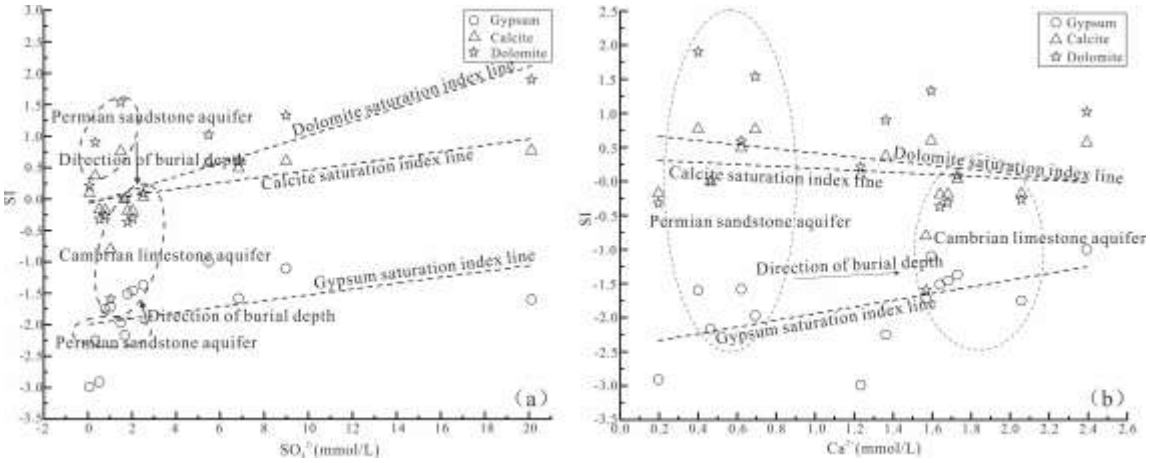

Figure 3. Saturation Indices and Hydrochemical Ionic Relationships of Gypsum, Calcite, and Dolomite

4.2. Temporal Distribution Characteristics of Sulfate

To investigate the impacts of long-term coal mining on sulfate concentrations across aquifers in the study area, sulfate concentration data from 2016 to 2024 were collected and visualized as bar charts[14,15,16,17,18,19]. As shown in Figure 4, sulfate concentrations in the phreatic aquifer remained relatively stable (around 200 mg/L) except for a notable decrease in 2017, indicating minimal

influence from coal mining and human activities on phreatic groundwater sulfate. In the sandstone aquifer, sulfate concentrations generally increased over the mining period; however, abnormally low values occurred between 2018 and 2021, followed by a sharp rise from 2021 to 2024, suggesting distinct mechanisms driven by prolonged mining activities during these two intervals. In the limestone aquifer, sulfate concentrations fluctuated dynamically but predominantly stabilized near 200 mg/L. In summary, influenced by long-term mining activities, sulfate variations in the study area exhibit complex spatiotemporal patterns across aquifers, necessitating further systematic investigation.

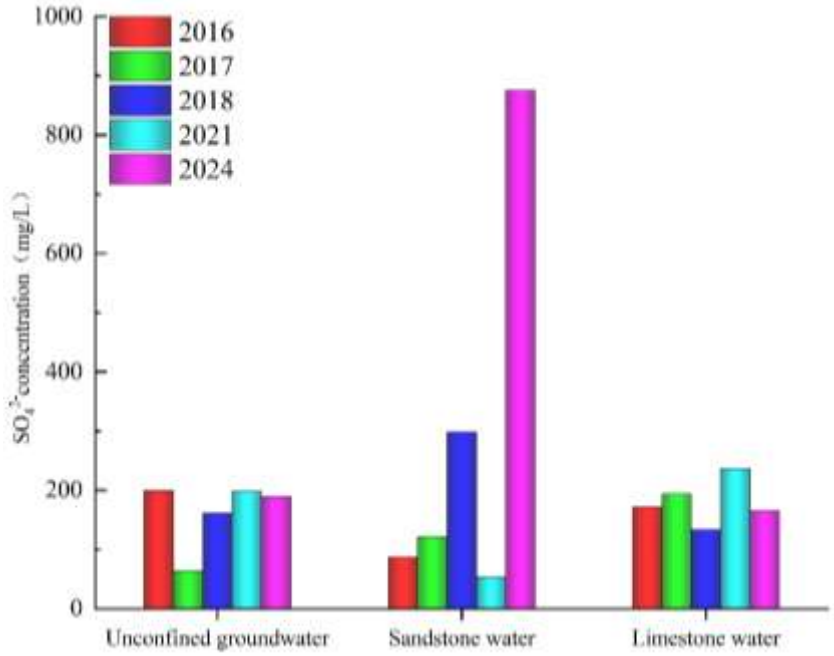

Figure 4. Temporal Variation of Sulfate in the Study Area

4.3. High Geotemperature Environment

Scholars have studied magmatic rock heat production in the Pingdingshan coal mining area through radioactive activity concentrations (uranium, thorium, and potassium), finding that the average geothermal gradient of the Pingdingshan coalfield is 3.32°C/100 m. At a burial depth of 1000 m, the temperature of rocks or groundwater can reach up to 49.57°C, representing a significantly higher geotemperature anomaly compared to other regions in Henan Province[20]. As shown in Figure 5, sulfate concentrations in the Pingdingshan and Jiaozuo coal mining areas share similar minimum values but exhibit significant differences in distribution ranges and mean values. In the Jiaozuo coal mining area, sulfate concentrations range from 7.91 mg/L to 67.87 mg/L, primarily distributed between 30 mg/L and 70 mg/L, with a mean value of 44.175 mg/L and a maximum value of 67.87 mg/L. In contrast, sulfate concentrations in the Pingdingshan coal mining area range from 7.09 mg/L to 526.26 mg/L, primarily distributed between 70 mg/L and 200 mg/L, with a mean value of 184.66 mg/L.In aquifers, mineral dissolution[21], sulfide oxidation, and bacterial sulfate reduction are all influenced by temperature. For example, in aerobic environments, sulfide oxidation rates increase by 3–5 times for every 20 K temperature rise; in anaerobic environments, sulfide oxidation rates increase by 2–11 times for every 30 K temperature increase [43]. Additionally, when temperatures reach levels suitable for rapid growth of sulfate-reducing bacteria (SRB), bacterial sulfate reduction accelerates, leading to decreased sulfate concentrations in groundwater. The anomalously high sulfate concentrations in the Pingdingshan coal mining area's groundwater may result from the high geotemperature environment, which intensifies water-rock interactions and sulfide oxidation in limestone aquifers, thereby causing elevated sulfate concentrations and widespread distribution.

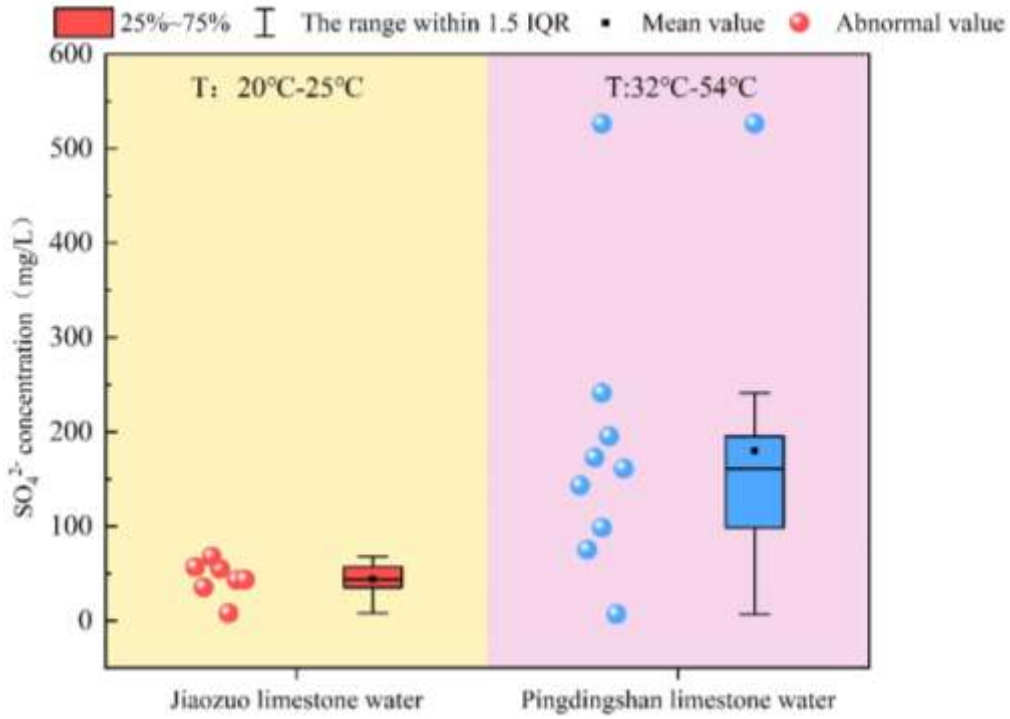

Figure 5. Temperature and Sulfate Relationship Diagram

5. CONCLUSIONS

The groundwater SO_4^{2-} concentrations in the study area exhibit significant variations influenced by multiple factors. Due to abnormally high geotemperature and prolonged mining activities, the groundwater environment has become highly complex. To clarify the sources and evolution of groundwater SO_4^{2-}, this study analyzed sulfate migration and transformation processes in high geotemperature coal mining areas through hydrochemical methods, yielding the following conclusions:

(1) Ion ratio analyses reveal that hydrochemical components in the groundwater are predominantly controlled by cation exchange, while sulfate in limestone groundwater primarily originates from gypsum dissolution. Combined with saturation indices, mining activities disrupt reducing environments, triggering sulfide oxidation in aquifers and generating H^+. Concurrently, intense cation exchange reduces Ca^{2+} concentrations, accelerating gypsum dissolution.

(2) Sulfate concentrations in the sandstone aquifer, influenced by long-term mining, show the most pronounced variations. Between 2021 and 2024, sulfate concentrations increased by nearly 800 mg/L, indicating that prolonged mining intensifies water-rock interactions, alters aquifer redox conditions, and exacerbates evaporite dissolution and sulfide oxidation.

(3) High geotemperature environments enhance sulfide oxidation and evaporite dissolution in groundwater, resulting in significantly higher SO_4^{2-} concentrations compared to normal-temperature coal mining areas.

CONFLICTS OF INTEREST

The authors declare that they have no conflict of interest.

REFERENCES

[1] Zhang Yanpeng. Implications of multi-isotope for geochemical environment evolution of groundwater in Shijiazhuang area [D]. china university of geosciences,2016.

[2] Singh A K and Sahu J N, 2018. Coal mine gas: a new fuel utilization technique for India. nternational [J]. Journal of Green Energy, 15, 732-743.

[3] Dong Donglin, Zhang Longqiang, Zhang Enyu, Fu Peiqi. Geochemical process and water quality evaluation of karst groundwater in the Baiquan $pring area under exploitation of coal and iron resources and inflow of southern water into Hebei Province [J/OL]. Journal of China Coal Society,1-22, 2025. DOI:10.13225/j.cnki.jccs.YG24.1517.

[4] Marove C A, Tangviroon P, Tabelin C B, et al, 2020. Leaching of hazardous elements from Mozambican coal and coal ash [J]. Journal of African Earth Sciences, 168, 103861.

[5] Marove C A, Sotozono R, Tangviroon P, et al, 2022. Assessment of soil, sediment and water contaminations around open-pit coal mines in Moatize, Tete province, Mozambique [J]. Environmental Advances, 8, 100215.

[6] Monjardin C E F, Senoro D B, Magbanlac J J M, et al, 2022. Geo-accumulation index of manganese in soils due to flooding in Boac and Mogpog Rivers, Marinduque, Philippines with mining disaster exposure [J]. Applied Sciences, 12 (7), 3527.

[7] Jin Menggui, Zhang Jie, Zhang Zhixin, Cao Mingda, Huang Xin. A review on source identification of dissolved sulfate in groundwater:Advances, problems and development trends [J]. Bulletin of Geological Science and Technology,2022,41(05):160-171. DOI:10.19509/j.cnki.dzkq.2022.0161.

[8] Acharya B S and Kharel G, 2020. Acid mine drainage from coal mining in the United States — an overview [J]. Journal of Hydrology, 588, 125061.

[9] Ding Fengfan. Water source discrimination model and hydrogeochemical simulation of typical North China type coalfield: A case study of No.13 mine in Pingdingshan Coal. DOI:10.27116/d.cnki.gjzgc.2021.000554 (2023).

[10] Zhao Y, Wang H, Wang J Q, Ma W J, Hou M X and Yang G X. Effects of Harvesting on Particulate Matter and Its Component Characteristics in Henan Wheat Region [J]. Chinese Journal of Inorganic Analytical, 13, 1444-1450. DOI:10.3969/j.issn.2095-1035.2023.12.025 (2023).

[11] Jiang X F. Studies on the Evolution Characteristics and the Controlling Factors of Hydrochemical Components in Pingdingshan Mining Area. DOI:10.27116/d.cnki.gjzgc.2020.000074 (2020).

[12] Li Xuexian. Study on hydrogeochemical characteristics and evolution rules of Karst basin under the effects of acid mine waste water [D]. Guizhou university,2019.

[13] Huang P H, Zhang Y N, Li Y M, Gao H F, Cui M K and Chai S W. A multiple isotope (S, H, O and C) approach to estimate sulfate increasing mechanism of groundwater in coal mine area. Science of The Total Environment. 900, 165852. https://doi.org/10.1016/j.scitotenv.2023.165852 (2023).

[14] Ding Fengfan. Water source discrimination model and hydrogeochemical simulation of typical North China type coalfield: A case study of No.13 mine in Pingdingshan Coal[D]. Henan polytechnic university. 2021.

[15] Huang P H, Cui M K, Chai S W, et al, 2024. Limestone water mixing process and hydrogen and oxygen stable isotope fractionation response under mining action [J]. Environmental Research, 255: 119208.

[16] Wang Xinyi, Zhao Wei, Liu Xiaoman, Wang Tiantian, Zhang Jiangguo, Guo Jianwei, Gen Guosheng, Zhang Bo. ldentification of water inrush source from coalfield based on entropyweight-fuzzy variable set theory [J]. Journal of China Coal Society,2017,42(09):2433-2439. DOI:10.16186/j.cnki.1673-9787.2023010018.

[17] Li Yanhe, Wu Zhanhui, Li Jiexiang, Yu Zhenzi, Zhang Bo, Wang Xinyi. The distribution characteristics and its influencing factors of rare earth elements in the karst geothermal water in Pingdingshan Coalfield [J]. Journal of Henan Polytechnic University(Natural Science),2025,44(01):88-99. DOI:10.16186/j.cnki.1673-9787.2023010018.

[18] Huang P, Yang Z, Wang X. et al, 2019. Research on Piper-PCA-Bayes-LOOCV discrimination model of water inrush source in mines [J]. Arabian Journal of Geosciences, 12, 334.

[19] Hu Y S, Huang P H, Gao H F, et al, 2022. State of the Practice Worldwide: HCA-PCA-EWM Discrimination Model of Water Inrush Source in Mines [J]. Groundwater Monitoring & Remediation, 42(2), 67-76.

[20] Zhou F X, Wu J H, Chen F J, et al, 2021. Using Stable Isotopes (δ18O and δD) to Study the Dynamics of Upwelling and Other Oceanic Processes in Northwestern South China Sea. JGR Oceans, 127(1).

[21] Migaszewski Z M, Gałuszka A, Michalik A, et al, 2013. The Use of Stable Sulfur, Oxygen and Hydrogen Isotope Ratios as Geochemical Tracers of Sulfates in the Podwiśniówka Acid Drainage Area (South-Central Poland) [J]. Aquatic Geochemistry, 19(4), 261-280.